Phase space control and consequences for cooling by using a laser-undulator beat wave

Yasuaki Kishimoto,[1,2] James K. Koga,[1] Toshiki Tajima,[1,3] and David L. Fisher[3]
[1]*Advanced Science Research Center, Japan Atomic Energy Research Institute, Ibaraki 311-01, Japan*
[2]*Naka Fusion Research Establishment, Japan Atomic Energy Research Institute, Ibaraki 311-01, Japan*
[3]*Department of Physics, The University of Texas at Austin, Austin, Texas 78712*
(Received 6 August 1996; revised manuscript received 17 January 1997)

We present a general method to control the phase space structure of charged particle beams by both Hamiltonian and non-Hamiltonian manipulations by employing multiple optical pulses. In particular, we focus on beam cooling as an example of the method. In order to rapidly cool a bunched beam of charged particles, one needs to introduce non-Hamiltonian manipulation of the internal structure of the phase space of the bunch. A spatially dependent force, which cancels the velocity moment fluctuations arising from the irregularity and granularity of the phase space, is shown to be effective in cooling the bunch. We introduce a method of cooling by creating a ponderomotive force due to a beat between a laser and an undulator that are appropriately adjusted turn by turn through feedback. If a high enough resolution feedback system can be achieved, this results in a rapid reduction of the longitudinal emittance of the bunch with a corresponding increase in the phase space of the scattered laser light. In this process we find that when the structure of the laser input is matched well with that of the beam, a large amount of entropy transfer without much energy transfer takes place (''entropy resonance''), while when it is ill matched, no such entropy resonance takes place. We measure the correlation dimension and higher entropy of the scattered laser light. It is found that both quantities are useful for determining the amount of cooling. By combining an appropriately timed Hamiltonian longitudinal beam stretching with the present cooling procedure, we can continue the cooling. Numerical simulation is carried out to demonstrate this method. [S1063-651X(97)08905-8]

PACS number(s): 29.27.Eg, 52.65.−y, 42.50.Fx

I. INTRODUCTION

In charged particle beam acceleration the primary goal has been the increase of energy itself. This is obvious, as the spatial resolution of matter Δr is related to the energy of the beam E by $\Delta r \sim \hbar c/E$. However, in addition to this, the improvement of beam quality, such as emittance reduction, is also important. The control of the phase space structure of the beam is thus the general problem we would like to address here. Phase space control includes cooling (phase space volume reduction), stochastic beam stacking [1], stochastic beam extraction [2], suppression of instabilities from multiple beam-beam interactions or head-tail effects [3], and beam phase space tailoring for advanced light sources [4]. For this paper we concentrate on cooling of charge particle beams as an example of an application of this method. The emittance ϵ of the beam is the phase space volume (or area) properly normalized. Thus its logarithm is related to the entropy of the beam. Emittance reduction is the problem of cooling. Cooling is not just a question of increasing the beam energy, but that of reducing the beam entropy.

Let us pose a question ''Can one cool a beam which obeys Hamiltonian dynamics, since electromagnetic fields can be written in Hamiltonian form?'' Electric fields (and magnetic fields) are functions of space only and not that of momentum. Upon application of an electric field on the beam, the area in phase space is unchanged. This illustrates the first kind of difficulty associated with cooling. Liouville's theorem states that a N-particle Hamiltonian system preserves phase space volume so that any external Hamiltonian electric or magnetic fields (time dependent or independent) would not cool a beam of N particles. The second kind of difficulty is, even if we succeed in applying a non-Hamiltonian interaction to the beam, the *second law of thermodynamics* dictates an increase, instead of a decrease, in the entropy, unless we do some extraordinary things.

In order to cool beams, therefore, one has to introduce some elements of non-Hamiltonianness into the system in a proper manner. Electron cooling of ions [5] and ionization cooling [6] are two methods that insert non-Hamiltonian processes and/or materials for the species of particles under consideration. Radiative cooling, such as with synchrotron radiation, is a classic non-Hamiltonian cooling method [7]. The now popular method of laser cooling of atoms is based on manipulation of the internal structure of the atoms (having electrons circulating around the nucleus) and ultimately on the radiative energy loss by transition [8]. This method has been applied to cooling heavy ions in storage rings [9]. However, beams of charged particles, such as electrons, muons, and protons do not have an easily manipulated internal structure. The stochastic cooling method [10] was introduced to reduce the phase space volume of hadron beams where other cooling methods are ineffective by feedback. The recently proposed faster optical stochastic cooling method [11] has been proposed for cooling lepton beams. In these methods the feedback operates on the average positional deviation of these particles.

In order to find out how to break this difficulty and to find a pathway to cooling, we consider a N-particle system in which the number of particles is conserved. Define a 6 N-dimensional phase space (the so-called Γ space) probability distribution function $\mathcal{D}(q_1, \ldots, q_N, p_1, \ldots, p_N; t)$, the Liouville distribution function. The conservation of particles

implies that the continuity equation in the $6N$-dimensional phase space

$$\frac{\partial \mathcal{D}}{\partial t}+\nabla\cdot(\mathbf{u}\mathcal{D})=0, \tag{1}$$

where $\mathbf{u}=(\{\dot{q}\}_N,\{\dot{p}_i\}_N)$ is the $6N$-dimensional phase space flow velocity and $\nabla=(\{\partial q_i\},\{\partial p_i\})$ is the $6N$-dimensional phase space gradient. If the flow in the $6N$-dimensional phase space is incompressible, or equivalently, $\nabla\cdot\mathbf{u}$ which is familiar for the condition of incompressibility in fluid mechanics, we have

$$\frac{\partial \mathcal{D}}{\partial t}+\mathbf{u}\cdot\nabla\mathcal{D}=0. \tag{2}$$

This is usually called the Liouville equation. The phase space incompressibility condition can be satisfied by the Hamiltonian dynamics. (Hamiltonianness is a sufficient but not necessary condition.) In order to derive a basic equation which is suitable for cooling problems, general equations of motion for the particles can be expressed as [12]

$$\dot{p}_i=X(i)+\sum_j F(i,j), \tag{3}$$

$$\dot{q}_i=Y(i)+\sum_j G(i,j), \tag{4}$$

where X,Y represent external forces and F,G represent interparticle forces as well as self-interaction forces.

Integrating Eq. (1) over $q_2p_2-q_Np_N$ and introducing $f_2=f_1f_1+g(q_1,p_1,q_2,p_2;t)$, where g is the intrinsic two-body correlation function, yields an equation for a one-body distribution which can be written as [12]

$$\begin{aligned}\frac{\partial f_1}{\partial t}&+\frac{\partial[X(1)f_1]}{\partial q_1}+\frac{\partial[Y(1)f_1]}{\partial p_1}\\&+N\frac{\partial f_1}{\partial q_1}\int dq_2dp_2F(1,2)f_1(q_2,p_2,t)\\&+N\frac{\partial f_1}{\partial p_1}\int dq_2dp_2G(1,2)f_1(q_2,p_2,t)\\&=-\frac{\partial[F(1,1)f_1]}{\partial q_1}-\frac{\partial[G(1,1)f_1]}{\partial p_1}\\&-N\int dq_2dp_2F(1,2)\frac{\partial g(q_1,p_1,q_2,p_2,t)}{\partial q_1}\\&-N\int dq_2dp_2G(1,2)\frac{\partial g(q_1,p_1,q_2,p_2,t)}{\partial p_1}.\end{aligned} \tag{5}$$

The terms on the left-hand side (LHS) are consistent with incompressible fluid flow. The first two terms on the right-hand side (RHS) are non-Hamiltonian self-interaction terms, such as radiation [7] or feedback [10]. The feedback may be looked upon as a time-retarded self-interaction, as the monitored particle memory in the (nearly) collisionless system will be fed on itself through the pickup circuit. The third and fourth terms represent microcorrelations among the particles. A similar more involved equation for the intrinsic two-body correlation function g can also be obtained (see [12]).

Typically the one-body entropy, which is defined as

$$S_1=-\int dq_1dp_1f_1\ln f_1, \tag{6}$$

is used to determine whether cooling or heating has occurred. This is the conventional entropy and is related to the logarithm of the emittance ϵ. Here we can define a higher nth order entropy [13] as

$$S_n=-\int dq_1dp_1\ldots dq_ndp_nf_n\ln f_n, \tag{7}$$

where f_n is the n body distribution function, $f_n(q_1,p_1,\ldots,q_n,p_n)$ derived from $\mathcal{D}$. The higher-order entropies are seldom studied in physics. It is important to understand the properties of the laws that govern these quantities. In fact it seems imperative to develop such theory for the physics of the quality of energy and for a more sophisticated modern information science. In such a theory the interplay of various entropies at different hierarchies should play an important role.

In Sec. II we discuss a basic idea on how to cool a bunch by introducing a spatially dependent force that cancels the fluctuations through feedback. The method of laser-undulator beat cooling is introduced in Sec. III. In Sec. IV we demonstrate this method by a one-dimensional (1D) numerical simulation and discuss its limitations. We also examine the properties of the laser light scattered from the beam. In the final section (Sec. V) we summarize our results and discuss the relationship between this light and the previously mentioned higher-order entropies. We also discuss future areas of research.

II. COOLING BY A SPATIALLY DEPENDENT FORCE

Here, we consider a method to realize the control and cooling of the charged particle system discussed in Sec. I. When we study the cooling of a charged particle system, the introduction of the discrete nature of the particles is essential. As an example in which cooling can be accomplished, consider a two-particle system. The discrete nature due to a finite number of particles leads to fluctuations that allows us to get a handle on the ''texture'' of phase space to compress it. In other words, the cooling mechanism involves ''compressing the vacuum between particles,'' which does not contradict Liouville's theorem as it assumes a (nearly) continuous phase space. This can be realized by applying a force that reduces the ''distance'' between these particles in phase space. This is trivially accomplished for a two-particle system by a *spatially* dependent *force* which accelerates the particle with lower momentum and decelerates the other particle to bring them both to a zero momentum difference (see Fig. 1). By doing so, although the mutual spatial distance remains as before, the mutual momentum distance collapses and the overall phase space distance (or one may call the effective ''emittance'' of this system) reduces. Of course a key ingredient is that cooling is only achieved when we have information concerning the positions of the particles. An arbitrary spatially dependent force where we do not know the particle

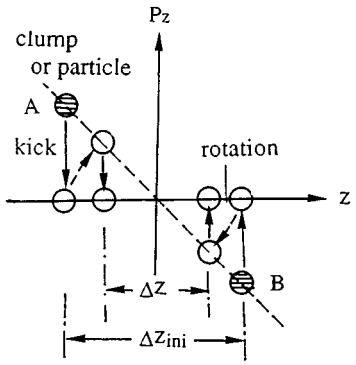

FIG. 1. Schematic picture of cooling in two particle (or clump) system (A,B). Δz_{ini} represents the initial real space spread and, by repeating the procedure of kick and rotation, two particles (or clumps) can approach each other to an order of the scale length of the kick field.

positions would not cool and most likely heat the system.

One can generalize this method to a system of N discrete particles or to a system with a continuous clumpy distribution of momentum fluctuation. This is done by a spatially dependent instantaneous application of a force $F_z(z)$ or equivalently an electric field $E_z(z)$, as shown in Fig. 2, where the coordinate z represents the direction of cooling. The kick will move a slice of the distribution vertically in the phase space (parallel to the momentum direction). The kick method might be considered an extension of van der Meer's stochastic cooling method [10] applied to a bunched beam. We consider utilization of a laser for this cooling method, because the wavelength of microwave radiation is too long to apply to short bunched beams like those in electron or positron storage rings. We show here a mathematical procedure to produce a spatially dependent electric field $E_z(z)$ from the fluctuation pattern of the beam distribution.

The method of cooling in real space (z direction) exchanges phase space elements by application of a spatially resolved force $F_z(z,t)=qE_z(z,t)$. Let us consider the cooling of a 1D system with distribution f_0 that is non-Maxwellian (including *clumpy* distribution). The total distribution f is

$$f(z,v,t)=f_0(z,v)+\delta f(z,v,t), \tag{8}$$

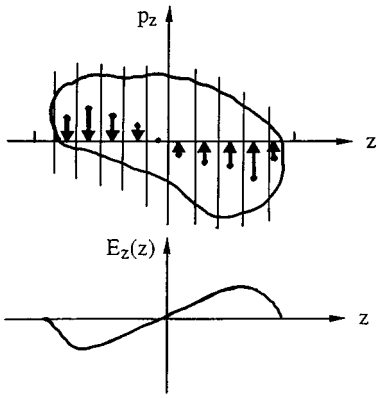

FIG. 2. Momentum kick.

where $\delta f(z,v,t=0)=0$, and $f_0(z,v)$ is the distribution measured before the application of the electric field $E_z(z,t)$. We require that the first velocity moment of the distribution $f(z,v,t)$ after application of $E_z(z,t)$ vanishes; $\langle v_f\rangle \equiv \int v f(z,v,t)dv=0$. This leads to the relation

$$\langle v_0\rangle=-\langle v\rangle, \tag{9}$$

where $\langle v_0\rangle=\int v f_0 dv$ and $\langle v\rangle=\int v\,\delta f dv$. The distribution δf in Eq. (8), as a result of the application of $E_z(z,t)$, is obtained as follows:

$$\frac{\partial f_0}{\partial t}+v\frac{\partial f_0}{\partial z}+\frac{qE}{m}\frac{\partial f_0}{\partial v}+\frac{\partial \delta f}{\partial t}+v\frac{\partial \delta f}{\partial z}+\frac{qE}{m}\frac{\partial \delta f}{\partial v}=0. \tag{10}$$

We linearize this equation with the first term being zero, dropping the last term, and transforming to Fourier-Laplace space

$$\frac{ikv}{s}\tilde{f}_0(k,v)+\frac{q}{m}\mathcal{FL}\left(E(z,t)\frac{\partial f_0(z,v)}{\partial v}\right)+s\,\widetilde{\delta f}(k,v,s) - \delta f(k,v,t=0)+ikv\,\widetilde{\delta f}(k,v,s)=0, \tag{11}$$

where $\mathcal{F}$ denotes the Fourier transform, $\mathcal{L}$ denotes the Laplace transform, $\widetilde{\delta f}(k,v,s)$ is the Fourier-Laplace transform of $\delta f(z,v,t)$ and $\delta f(k,v,t=0)=0$. Using $\mathcal{L}[E(z,t)]=E(z)/s$ [if $E(z,t)=E(z)$ for $t>0$ and $E(z,t)=0$ for $t<0$] and solving for $\widetilde{\delta f}(k,v,s)$, we have

$$\widetilde{\delta f}(k,v,s)=-\frac{1}{s(s+ikv)} \times\left\{\frac{q}{m}\mathcal{F}\left(E(z)\frac{\partial f_0(z,v)}{\partial v}\right)+ikv f_0(k,v)\right\}. \tag{12}$$

The inverse Fourier-Laplace transform yields

$$\delta f(z,v,t)=-\frac{q}{m}\mathcal{F}^{-1}\left\{\frac{1-\exp(-ikvt)}{ikv}\mathcal{F}\left(E(z)\frac{\partial f_0(z,v)}{\partial v}\right)\right\} -\mathcal{F}^{-1}\{f_0(k,v)[1-\exp(-ikvt)]\}, \tag{13}$$

where $\mathcal{F}^{-1}$ is the inverse Fourier transform. The impulse approximation means $t\to 0$, which yields $1-\exp(-ikvt)\to ikvt$. Therefore, the distribution after a kick (an impulse) is obtained as

$$\delta f(z,v,t)=-\mathcal{F}^{-1}\left\{\frac{q}{m}t\mathcal{F}\left(E(z)\frac{\partial f_0(z,v)}{\partial v}\right)\right\} -\mathcal{F}^{-1}\{f_0(k,v)ikv\}t =-\frac{q}{m}tE(z)\frac{\partial f_0(z,v)}{\partial v}-vt\frac{\partial f_0(z,v)}{\partial z}. \tag{14}$$

We impose our condition for feedback $\langle v_0\rangle=-\int v\,\delta f dv$. This leads to the expression

$$\langle v_0\rangle = \frac{q}{m} tE(z) \int v \frac{\partial f_0(z,v)}{\partial v} dv + t \int v^2 \frac{\partial f_0(z,v)}{\partial z} dv, \tag{15}$$

where t is the pulse duration. We solve for expression of the needed electric field $E(z)$ in order to make $\langle v_0\rangle = -\langle v\rangle$, obtaining

$$E(z) = -\frac{m}{qt}\frac{\langle v_0\rangle}{\langle n_0\rangle} + \frac{m}{q}\frac{1}{\langle n_0\rangle}\int v^2 \frac{\partial f_0(z,v)}{\partial z} dv. \tag{16}$$

For impulse $E(z)$ application $t \to 0$, the first term dominates and, thus, we obtain

$$E(z) = -\frac{m}{qt}\frac{\langle v_0\rangle}{\langle n_0\rangle}, \tag{17}$$

where $\langle v_0\rangle$ and $\langle n_0\rangle$ are functions of z.

III. BASIC EQUATIONS FOR THE LASER-UNDULATOR COOLING METHOD

In this section, we present the mathematical procedure of the laser-undulator cooling method presented in the preceding section. In Sec. III B, we derive the basic equations which describe the self-consistent beat wave kick for the cooling. Based on the equations in Sec. III B, we present a method to determine the external laser fields from the observed beam information in Sec. III C. We also discuss the conditions for providing an ideal kick which leads to efficient beam cooling.

A. Idea of cooling by using a laser-undulator beat wave

The crucial question is how to realize a spatially dependent correction force on a bunch particles. For most lepton storage rings, the necessary spatial resolution is far below microwave technology. An electric field $E_z(z) = F_z(z)/q$ (q : charge of particle) would be electrostatic and not practical as an accelerator feedback component. Furthermore, the force has to travel with the beam particles so as to be always in phase with the fluctuation pattern $\langle v_z\rangle(z)$ of the beam during the kick. To realize such a force, we suggest the method of the ponderomotive beat wave force [14] produced by a linear undulator and a laser with a broadband spectrum which is injected coparallel to the beam.

The basic idea of this method is as follows. The coupling between a laser field with frequency and wave number (ω_1, k_1) and an undulator with $k_w (\equiv 2\pi/\lambda_w)$ (λ_w : undulator pitch) produces a traveling ponderomotive potential parallel to the beam. The resonance condition of the ponderomotive potential with a beam particle of energy γ is given by

$$k_1 = \frac{2\gamma^2}{1+\hat{K}^2} k_w, \tag{18}$$

where $\hat{K} \equiv eB_w/\sqrt{2}mck_w$ (B_w : undulator magnetic fields) is the so-called K parameter. We choose k_1 and k_w as $2\pi/(k_1 + k_w) \simeq l_b$ (l_b : bunch length of the beam) so that the beam bunch is trapped in the ponderomotive potential well. When the dispersion relation Eq. (18) is satisfied for the frequency and corresponding wave number (ω_1, k_1), it is known that odd higher harmonics of the fundamental laser $\{(\omega_m \equiv m\omega_1, k_m),\ m = 3,5,7\cdots 2n+1\}$ also become resonant modes. This feature is shown in Fig. 3. This is due to the nonlinearity of the field amplitude which originates from the longitudinal oscillation with 1/2 wiggler period. Therefore, by precisely choosing the amplitude and phase of these higher harmonic lasers as well as the interaction length, we can realize an arbitrary spatially dependent field pattern traveling with the beam particles. We let the laser carry the precise detailed information necessary to manipulate the internal phase space structure and the undulator provide a strong beat wave field without energy loss. A Bose condensated laser usually containing little entropy (typically $S_l \sim k_B \ln 10$ close to the squeezed state or with little information) can wash out the much higher entropy of a charged particle beam (typically $S_b \sim k_B \ln 10^{10}$) with appropriately configured and repeated photon-particle interactions.

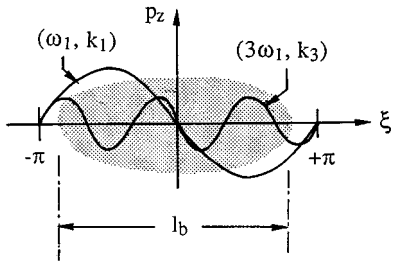

FIG. 3. Odd higher harmonics of the fundamental laser $\{(\omega_m \equiv m\omega_1, k_m),\ m = 3,5,7\cdots 2n+1\}$ are resonant modes which can also kick a beam in longitudinal phase space.

The overall features of beam cooling in a storage ring system is schematically shown in Fig. 4. Phase space information of the beam (more precisely in this case, the longitudinal fluctuation pattern) is extracted at the pickup section. Based on the extracted information, laser fields which have proper spectrum shape (like amplitude, phase, etc., . . .) are programmed through calculations, so that the beam is cooled at the kicker section after the interaction. The laser fields (or superimposed laser wave packet) is transmitted to undulator

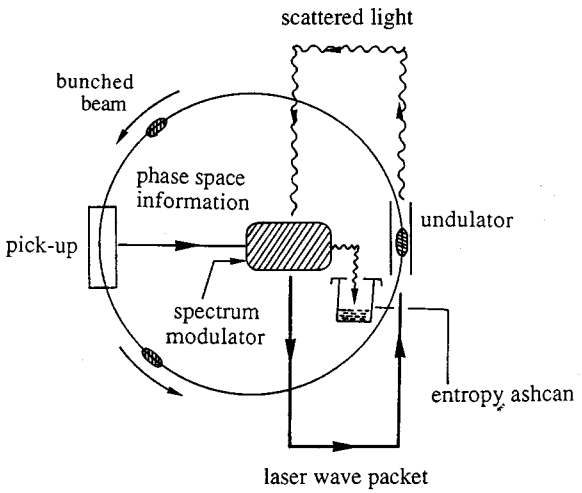

FIG. 4. Overall picture of laser-undulator beat wave cooling in storage ring system.

(or kicker) by adjusting the phase with the beam orbit and kicks the bunched beam. During the interaction, the beam entropy is extracted by the laser fields. Namely, the scattered laser entropy (i.e., photon entropy) should increase when the incident laser correctly kicks the beam. This exchange of entropy between the bunched beam and laser fields is actually observed in our numerical cooling simulation and is discussed in Sec. IV. It is also found that after interaction the total power consumption of laser fields is extremely small (almost zero). Namely, although a certain amount of laser power is needed to form the kick field, once the power is supplied to the laser system, the scattered laser light can be recycled for the next kick, as shown in Fig. 4 by reprogramming the spectrum based on new information. During the reprogramming process, the increased laser entropy is thrown away from the system.

B. Basic equations

We investigate the present cooling method by employing a one-dimensional linear undulator model which describes the self-consistent interaction between beam particles and laser fields in the longitudinal z direction [15]. We start from the situation where the laser fields $\mathbf{A}_s$ and the undulator field $\mathbf{A}_w$ used for cooling the beam are given by

$$\mathbf{A}_s(z;t)=\sum_m A_m(z)\sin\psi_m(z,t)\hat{\mathbf{e}}_y, \tag{19}$$

$$\mathbf{A}_w(z)=A_w\sin k_w z\hat{\mathbf{e}}_y, \tag{20}$$

where the phase of the laser, ψ_m, is given by

$$\psi_m(z,t)=\int_0^z k_m(z')dz'-\omega_m t+\delta_m. \tag{21}$$

Here, $\omega_m=m\omega_1$ (m: integer) is the angular frequency of the higher harmonics with respect to the fundamental angular frequency ω_1. k_m and δ_m represent the corresponding wave number and initial laser phase. The Hamiltonian from which the equation of motion is derived is described by taking z as the independent variable

$$K=-\sqrt{(\gamma^2-1)m^2c^2-[\hat{\mathbf{p}}_\perp-(e/c)(\mathbf{A}_s+\mathbf{A}_w)]^2}, \tag{22}$$

where $\hat{\mathbf{p}}_\perp=(\hat{p}_x,\hat{p}_y)$ is the transverse canonical momentum which are given by $\hat{p}_x=0$ and $\hat{p}_y=-\hat{K}mc\sin k_w z$ in this case. In Eq. (22), we neglected the space charge field. The above Hamiltonian is equivalent to $K=-\hat{p}_z=-\gamma mv_z$ ($\hat{p}_z$: the canonical momentum in z direction) and $\beta_z=v_z/c$ is given by

$$\beta_z\simeq\left(1-\frac{1+\hat{K}^2}{\gamma^2}+\frac{\hat{K}^2}{\gamma^2}\cos 2k_w z\right)^{1/2}. \tag{23}$$

The equation of motion is derived from $d\gamma/dz=(1/mc^2)\partial K/\partial t$ as

$$\frac{d\gamma}{d\hat{z}}=\frac{mca_w}{2K}\sum_m a_m\hat{k}_{m0}(\sin\tilde{\psi}_m^{(+)}-\sin\tilde{\psi}_m^{(-)}), \tag{24}$$

$$\tilde{\psi}_m^{(\pm)}(z,\psi)=\psi_m-(m\mp 1)k_w z-\alpha_m\sin 2k_w z, \tag{25}$$

where $\psi_m=m\tilde{\psi}+\phi_m(z)+\delta_m$, $a_w=eA_w/mc^2(=\sqrt{2}\hat{K})$, $a_m=eA_m/mc^2$, $\hat{z}=k_w z$, $\hat{k}_{m0}=\omega_m/ck_w$, and $\alpha_m=\hat{k}_{m0}\hat{K}^2/4\gamma^2$. Here, $\tilde{\psi}$ represents the phase of a particle with respect to the fundamental ponderomotive field which satisfies the equation

$$\frac{d\tilde{\psi}}{d\hat{z}}=1-\frac{\hat{k}_{10}}{2\gamma^2}(1+\hat{K}^2), \tag{26}$$

with the initial condition $\tilde{\psi}(\hat{z}=0)=-\omega_1 t_0(\equiv\psi)$, where t_0 denotes the time that a particle is located at $\hat{z}=0$. $\phi_m(z)$ represents the shift of the laser phase due to the finite beam current which satisfies

$$\frac{d\phi_m}{d\hat{z}}=\hat{k}_m-\hat{k}_{m0}(\equiv\delta\hat{k}_m), \tag{27}$$

with the initial condition $\phi_m(\hat{z}=0)=0$. Equation (24) is a nonlinear equation with respect to the laser amplitude a_m due to the longitudinal oscillation of the particle with period π/k_w in the ponderomotive phase. This nonlinearity in the laser amplitude allows resonance with odd higher harmonics $(3\omega_1,5\omega_1,7\omega_1,\ldots)$. This is seen by taking the average of Eq. (24) over the wiggler period. The even harmonic numbers are found to cancel out and we are led to

$$\frac{d\gamma}{d\hat{z}}=-\frac{a_w}{2\beta_{z0}\gamma}\sum_{m(\text{odd})} a_m\hat{k}_{m0}G_m(\alpha_m)\sin\psi_m, \tag{28}$$

where $G_m(\alpha_m)=J_{(m-1)/2}(\alpha_m)-J_{(m+1)/2}(\alpha_m)$, $\beta_{z0}=\sqrt{1-(1+\hat{K}^2)/\gamma^2}$, and m is taken to be an odd number. Here, t_0 which gives the initial condition for Eq. (26) ranges between $-\pi/\omega_1\leqslant t_0\leqslant\pi/\omega_1$.

The transverse current of the beam is described by

$$\mathbf{J}_\perp(z,t)=-en_b v_b\int_{-\infty}^{+\infty}\frac{v_x(t,t_0)}{v_z(t,t_0)}\delta[t-\tau(z,t_0)]dt_0\hat{\mathbf{e}}_x, \tag{29}$$

where $v_b=c\sqrt{1-(1+\hat{K}^2)/\gamma_b^2}$, $\gamma_b=1+E_b/mc^2$ (E_b: the beam energy), n_b the average beam density, $\tau(z,t_0)=t_0+\int_0^z(1/v_z)dz$, and $\mathbf{v}_\perp(t,t_0)$ the velocity of an electron at time t which enters the interaction region at $t=t_0$. Then, the field equations which govern the field amplitude a_m and the phase shift ϕ_m are derived from the Maxwell's equation in terms of the above nonlinear current as follows:

$$\frac{da_m}{d\hat{z}}=\frac{\gamma_b\beta_b\xi^2}{2\hat{k}_{m0}}a_w\left\langle\frac{\sin\tilde{\psi}_m^{(+)}-\sin\tilde{\psi}_m^{(-)}}{\beta_z\gamma}\right\rangle, \tag{30}$$

$$\frac{d\phi_m}{d\hat{z}}=\frac{\gamma_b\beta_b\xi^2}{2\hat{k}_{m0}}\frac{a_w}{a_m}\left\langle\frac{\cos\tilde{\psi}_m^{(+)}-\cos\tilde{\psi}_m^{(-)}}{\beta_z\gamma}\right\rangle, \tag{31}$$

where $\beta_b\equiv v_b/c$, $\xi\equiv\omega_b/\sqrt{\gamma_b}ck_w$, and $\omega_b\equiv\sqrt{4\pi n_b e^2/m}$. $\langle A\rangle=(1/2\pi)\int_{-\pi}^{+\pi}Ad\psi$ represents the average of the beam

particles over the fundamental ponderomotive phase. Then, by taking the wiggler average, Eqs. (30) and (31) reduce to

$$\frac{da_m}{d\hat{z}}=\frac{\gamma_b\beta_b\xi^2}{2\hat{k}_{m0}}a_w\left\langle\frac{G_m\sin\psi_m}{\beta_z\gamma}\right\rangle, \tag{32}$$

$$\frac{d\phi_m}{d\hat{z}}=\frac{\gamma_b\beta_b\xi^2}{2\hat{k}_{m0}}\frac{a_w}{a_m}\left\langle\frac{G_m\cos\psi_m}{\beta_z\gamma}\right\rangle. \tag{33}$$

The set of Eqs. (26), (28), (30), (31) [or (32), (33)] describe the self-consistent interaction between the multifrequency laser fields and the beam particles which is essentially the same as the free-electron laser (FEL) description.

In deriving Eqs. (30) and (31), we assumed periodic boundary conditions for the fundamental ponderomotive phase $\tilde{\psi}$. Therefore, the beam density n_b in Eq. (29) is given by $n_b=N/\lambda_p$, where N is the particle number per bunch and $\lambda_p=2\pi/(k_{10}+k_w)$ is the wave length of the fundamental ponderomotive potential. In the case of a storage ring which circumference is L, n_b is given in terms of the average beam current J_b as

$$n_b=\frac{J_b}{|e|v_b}\frac{L}{\lambda_p M_b}, \tag{34}$$

where M_b is the number of bunches in the ring.

C. Determination of the kick field

In this section, we provide the procedure to determine the laser amplitude and phase from the information of the fluctuation pattern of the beam bunch. Here, we begin by solving Eq. (28) order by order assuming the smallness parameter $\epsilon\sim|\gamma_{ini}-\gamma_{res}|/\gamma_{ini}\ll 1$, where $\gamma_{ini}=\gamma(z=0)$ is the initial particle energy and $\gamma_{res}=\sqrt{\hat{k}_{10}(1+\hat{K}^2)/2}$ is the resonant γ which satisfies $d\tilde{\psi}/d\hat{z}=0$. Keeping the zeroth order solution with respect to $\epsilon\sim|\delta\gamma|/\gamma_{ini}$ ($\delta\gamma\equiv\gamma_{ini}-\gamma_{res}$), by taking $\gamma=\gamma_{ini}$ and $\tilde{\psi}=\xi(=\text{const})$ on the RHS of Eq. (28), we simply obtain

$$\gamma^{(0)}(\hat{z};\xi)=\gamma_{ini}+\sum_{m(\text{odd})}F_m\sin(m\xi+\delta_m)\hat{z}, \tag{35}$$

where $F_m=-[a_w a_m\hat{k}_{m0}G_m(\gamma_{ini})/2\beta_z(\gamma_{ini})\gamma_{ini}]$. The solution up to the first order with respect to ϵ is obtained as follows. Equation (26), the phase of the test particle, is solved by employing the zeroth order orbit Eq. (35) as follows:

$$\tilde{\psi}\simeq\xi+\epsilon_1\hat{z}+\epsilon_2\hat{z}^2, \tag{36}$$

$$\epsilon_1=1-\frac{\hat{k}_{10}(1+\hat{K}^2)}{2\gamma_{ini}^2}\sim\frac{2\delta\gamma}{\gamma_{res}}\sim\mathcal{O}(\epsilon), \tag{37}$$

$$\epsilon_2=\frac{\hat{k}_{10}(1+\hat{K}^2)}{2\gamma_{ini}^2}\frac{f(\xi)}{\gamma_{ini}}\simeq\left(1-\frac{2\delta\gamma}{\gamma_{res}}\right)\frac{f(\xi)}{\gamma_{ini}}\simeq\frac{f(\xi)}{\gamma_{res}}, \tag{38}$$

where $f(\xi)=\Sigma_m F_m\sin(m\xi+\delta_m)$. The third term on the RHS in Eq. (36) represents the deviation from the straight motion of $\tilde{\psi}$ (and then γ) during the kick. Note that since $f(\xi)$ is chosen so that $f(\xi)\hat{z}\simeq\delta\gamma$ from Eq. (35), $\epsilon_2\simeq f(\xi)/\gamma_{ini}\simeq(\delta\gamma/\gamma_{ini})\hat{z}\simeq\epsilon$ when the interaction length $\hat{z}$ is chosen $\hat{z}\sim 1$. By substituting Eq. (36) into Eq. (28), we are led to a solution up to first order in ϵ as follows:

$$\gamma(\hat{z},\tilde{\psi};\xi)=\gamma_{ini}+\sum_{m(\text{odd})}F_m\left[\hat{z}\sin(m\xi+\delta_m)+\left(\frac{m}{2}\epsilon_1\hat{z}^2+\frac{m}{3}\epsilon_2\hat{z}^3+\frac{\delta k_m}{2}\hat{z}^2\right)\cos(m\xi+\delta_m)\right], \tag{39}$$

where we assumed that the shift of the laser phase ϕ_m is simply estimated by $\phi_m\simeq\delta k_m\hat{z}\leqslant\mathcal{O}(\epsilon)$. As we discussed above, since $f(\xi)=-\delta\gamma/\hat{z}$ and $\epsilon_2\hat{z}^3\simeq-(\delta\gamma/\gamma_{res})\hat{z}^2$, then Eq. (39) is rewritten as

$$\gamma(\hat{z},\tilde{\psi};\xi)=\gamma_{ini}+\sum_{m(\text{odd})}F_m\left\{\hat{z}\sin(m\xi+\delta_m)+\left[\frac{2}{3}m\left(\frac{\delta\gamma}{\gamma_{res}}\right)+\frac{\delta k_m}{2}\right]\hat{z}^2\cos(m\xi+\delta_m)\right\}. \tag{40}$$

Here, we divide the fundamental ponderomotive phase into n slices in which the beam bunch is located as shown in Fig. 5. We assume that there are N_j particles in the jth slice and the total particle number in the bunch is $N=\Sigma_{j=0}^{n-1}N_j$. Let

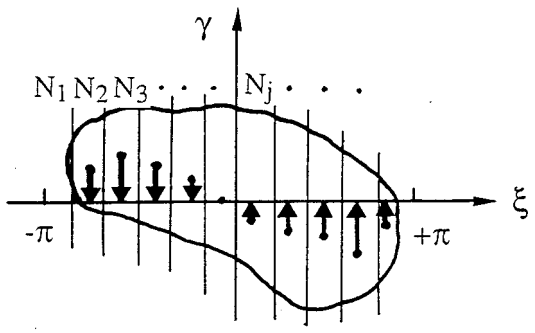

FIG. 5. The fundamental pondermotive phase broken up into n slices with N_j particles in the jth slice.

$$\langle\delta\gamma\rangle_j=\sum_{i=1}^{N_j}\frac{\gamma_i}{N_j}-\gamma_{res} \tag{41}$$

be the energy fluctuation in the jth layer which is in principle experimentally observable [16,17]. Here, the average γ, i.e., $\overline{\gamma}=(1/n)\Sigma_{j=0}^{n-1}\Sigma_{i=1}^{N_j}(\gamma_i/N_j)$ is identical to γ_{res} since the fundamental laser wave number $\hat{k}_{10}$ is determined by the relation $\hat{k}_{10}=2\overline{\gamma^2}/(1+\hat{K}^2)$. The laser amplitude and phase are determined from Eq. (35) by neglecting the change of the phase as follows. That is, by taking $\gamma(\hat{z},\xi)$ to γ_{res} and averaging Eq. (35) with respect to particles in each slice, we obtain

$$\langle \delta\gamma\rangle_j = \sum_{m(\mathrm{odd})} \langle H_m\rangle_j \sin(m\xi_j + \delta_m), \tag{42}$$

where $\xi_j = 2\pi j/n$ and $\langle H_m\rangle_j = -\Sigma_{i=1}^{N_j} F_m(\gamma_{ini,i})/N_j$. Here, $\langle H_m\rangle_j \simeq H_m(\gamma_{res})(\equiv -F_m(\gamma_{res})\hat{z})$ is assumed. Therefore, for the observed fluctuation profile $\langle \delta\gamma\rangle_j$ in each slice, the amplitude H_m and phase δ_m are determined through the Fourier transform relation. Note here that since the even harmonics are excluded in Eq. (42), the reconstruction of the fluctuation profile in terms of the Fourier amplitude and phase by employing only the odd harmonics is incomplete. However, the incompleteness can be minimized by the following discussion. The wave amplitude a_m and phase δ_m are obtained in terms of $H_m(\gamma_{res})$ and the interaction length, $\hat{z}$, as

$$a_m \simeq \alpha\left(\frac{2\overline{\beta_{z0}}\gamma_{res}\overline{H_m}}{a_w \hat{k}_{m0}\overline{G_m}\hat{z}}\right), \tag{43}$$

$$\delta_m = \tan^{-1}\left[\int_{-\pi}^{+\pi} \delta\gamma(\xi)\cos m\xi d\xi \Big/ \int_{-\pi}^{+\pi} \delta\gamma(\xi)\sin m\xi d\xi\right], \tag{44}$$

where $\overline{\beta_{z0}} = \beta_{z\,0}(\gamma_{res})$, $\overline{H_m} = H_m(\gamma_{res})$, and $\overline{G_m} = G_m(\gamma_{res})$. α is an adjustable parameter to let $\langle \delta\gamma\rangle_j$ tend to zero [18]. Due to the lack of even harmonics in the laser field, the coefficient α, which vanishes the fluctuations, is ideally given by 2, but adjustably chosen by taking into account the effect of the phase change. In Eq. (43) the laser amplitude is inversely proportional to $\hat{z}$ and can be reduced by taking a laser interaction length short. However, the amplitude as well as the interaction distance has to be chosen so that they satisfy the ideal kick condition, as discussed in Sec. III A.

D. Constraint for an ideal kick

Here, we consider several mechanisms which prevent beam kick from being ideal within the present framework. First, the second term on the RHS of Eq. (39) [or Eq. (40)] provides a limitation on the ideal kick condition. Since the kick field is determined by neglecting the terms which are proportional to $\cos(m\xi + \delta m)$ in Eq. (40), the deviation (or error) of the average energy of the jth layer from $\gamma = \gamma_{res}$ after the kick, $\Delta\gamma_{\mathrm{err}}$, is estimated by

$$\langle \Delta\gamma_{\mathrm{err}}\rangle_j = \sum_m F_m\left[\frac{2}{3}m\left(\frac{\langle \delta\gamma\rangle_j}{\gamma_{res}}\right) + \frac{\delta k_m}{2}\right]\hat{z}^2\cos(m\xi + \delta_m), \tag{45}$$

where $f(\xi)$ in Eq. (38) is estimated by $f(\xi) = -\langle \delta\gamma\rangle_j/\hat{z}$. The first term of the RHS in Eq. (45) represents the effect of ballistic phase change due to the mismatch between γ_{res} and the average particle γ in each layer. The second term represents the shift of the laser phase due to the finite current effect. In the small current limit where the laser amplitude a_m and phase ϕ_m are not changed during the kick, the condition for energy spread to realize an ideal kick (or cooling) by this method is given by

$$\frac{\langle \delta\gamma\rangle_b}{\gamma_{res}} \ll \frac{3}{2m\hat{z}}. \tag{46}$$

In obtaining Eq. (46) from Eqs. (42) and (45), we estimate $\langle \delta\gamma\rangle_j$ simply by $\langle \delta\gamma\rangle_b$, where $\langle \delta\gamma\rangle_j$ in Eq. (45) is estimated by the average beam energy spread $\langle \delta\gamma\rangle_b$. It is found that a shorter interaction distance allows a larger initial energy spread and large scale fluctuations, which have a small m number, also allow a larger energy spread. This result indicates that since $\langle \delta\gamma\rangle_b/\gamma_{res}$ becomes smaller with cooling, once the condition given by Eq. (46) is initially satisfied for the largest scale fluctuation, the small scale fluctuations which have the larger m number satisfy the condition Eq. (46) and can be continually cooled.

The kick of the beam is also modified through the change of the wave number of the laser field in the higher beam current and/or density case. The condition on the beam density for an ideal kick is also estimated from Eq. (46) and Eq. (33) as

$$\xi^2\left(\equiv\frac{\omega_b^2}{\gamma_b c^2 k_w^2}\right) \ll \frac{4\hat{k}_{m0}\gamma_b}{\hat{z}G_m}\left(\frac{a_m}{a_w}\right), \tag{47}$$

where $\langle\cos\psi_m\rangle \simeq 1$ is assumed in Eq. (33). By employing Eq. (43), we rewrite Eq. (47) as

$$n_b \ll \frac{4mc^2k_w^2}{\pi e^2}\frac{\gamma_b^2\overline{H_m}}{a_w^2 G_m^2 \hat{z}^2}, \tag{48}$$

where the density limit is proportional to $\gamma_b^2/\hat{z}^2$.

Once the fluctuations are eliminated by the above kick procedure for a particular turn, fluctuations are bound to be induced by the phase space rotation $\mathcal{M}(\mathcal{K};\mathcal{P})$. Additional inducement may come in through nonlinearities of the magnets and rf waves and through other Hamiltonian elements to (deliberately) induce fluctuations. Thus, the laser fields are adjusted turn by turn (or in a whatever necessary period) based on the induced fluctuation pattern to match Eqs. (43) and (44).

IV. NUMERICAL EXPERIMENTS

As a demonstration of the present cooling method, we show a numerical example in the case of a shortly bunched electron beam in this section. Typical beam parameters are the beam energy $E_{\mathrm{b}} = 200$ MeV ($\gamma_b \simeq 392$), the bunch length $l_b \leqslant 0.2$ cm, the initial beam energy spread $\Delta\gamma/\gamma_b \simeq 3\%$, and the beam current $J_b = 0.5$ A/cm^2 (the average current density in the storage ring, J_b, is given by $J_b = \overline{J_b}[(\lambda_p M_b)/L]$). From the bunch size, we determine the fundamental laser frequency as $\omega_1/2\pi = 150$ MHz so that $\lambda(\equiv 2\pi/\omega_1) \simeq l_b$. The undulator is designed so that $\lambda_w = 0.984$ m and $B_w = 3.85$ KG, where the corresponding $\hat{K}$ parameter is $\hat{K} \simeq 25$ and the interaction length is chosen to be $\hat{z} = \pi$ (half undulator pitch) in the present simulation. We initially provide the beam distribution f_{b} in the fundamental phase space according to

$$f_b(\gamma, \psi_0) = \frac{N}{2\pi\sigma_\psi\sigma_\gamma}\exp\left[-\frac{\psi_0^2}{2\sigma_\psi^2} - \frac{(\gamma-\gamma_b)^2}{2\sigma_\gamma^2}\right], \tag{49}$$

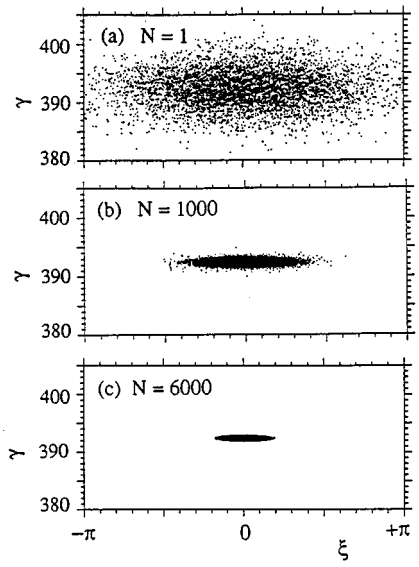

FIG. 6. Particle distribution plot in phase space at three different turn numbers. (A set of parameters, $E_b=200$ MeV, $\Delta\gamma/\gamma_{ini}\simeq 0.03$, $l_b\simeq 2$ mm, $\omega_1=150$ GHz, $\lambda_w=0.984$ m, $B_w=3.85$ kG ($\hat{K}\simeq 25$ and $\delta\hat{z}=\pi$ were chosen); for particle distribution (a) turn $N=1$, (b) $N=1000$, and (c) $N=6000$, respectively.

where σ_ψ and σ_γ are the standard deviation of the bunch in the phase and longitudinal energy directions and therefore $\sigma_\psi\sigma_\gamma$ represents the longitudinal emittance.

It should be noted that with the current simulation parameters and necessary resolution for cooling a resolution of ~ 30 μm or an equivalent bandwidth of ~ 10 THz is needed in the pickup or detector of an actual system. Although such resolution is not currently available, it may be possible via time of flight methods [11] or other means which we are currently investigating. We want to demonstrate the beat wave method as a proof of principle and examine the consequences for cooling in having such a system.

A. Beam phase space

Figure 6(a) shows the initial particle distribution in the fundamental phase space. First, we show the case in which the fundamental ponderomotive phase is divided into $n=128$ slices and $N_L=32$ odd harmonic lasers are employed. In the simulation, the beam bunch is kicked by the adjusted laser beat wave by the half undulator pitch so that the fluctuation inside the beam is minimized. The above kick process is repeated by renewing the laser fields turn by turn, modeling the storage ring as a simple Hamiltonian rotation in phase space. We assume in this simple model that the ring is dispersionless. In a real machine the dispersion among other effects plays an important role in the beam dynamics, but in this paper we concentrate on the interaction. A proper beam rotation in phase space is applied for each turn around the beam center to extract the fluctuation from the beam for the ψ_0 axis. The particle distribution and density contour plot after $N=1000$ turns and $N=6000$ turns are illustrated also in Figs. 6(b) and 6(c), respectively. It is found that the beam bunch is rapidly cooled down on a turn by turn basis both in the phase and energy directions. The turn number dependence of the normalized emittance $\widehat{\epsilon}\equiv\widehat{\sigma_\psi}\widehat{\sigma_\gamma}(=\sigma_\psi\sigma_\gamma/\pi\gamma_b)$ is shown in Fig. 7. The emittance is rapidly reduced with turns almost following an exponential dependence up to $N\simeq 1000$–1500 and then the cooling rate becomes smaller. At around $N=6000$ turns, the emittance is found to be reduced to about 1/50th of the initial one.

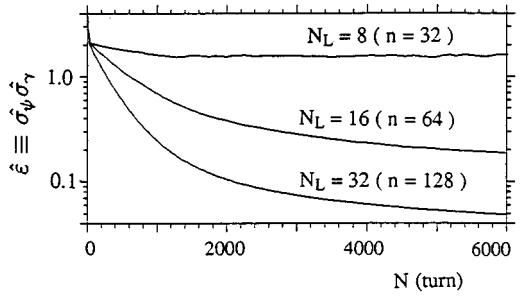

FIG. 7. Emittance $\hat{\varepsilon}\equiv\sigma_\psi\sigma_\gamma/\pi\gamma_b$ as a function of turn N for slice number $N_L=32$, $N_L=16$, and $N_L=8$.

Figures 8(a) and 8(b) show the fluctuation pattern $\langle\delta\gamma\rangle_j/\overline{\gamma}$, before and after the kick at $N=1000$ turns which corresponds to Fig. 6(b). The corresponding adjusted beat field to kick the beam and minimize the fluctuation given by Fig. 8(a) is shown in Fig. 9(a). The power spectrum of the laser field is also shown in Fig. 9(b). After the kick by the beat wave [Fig. 8(b)], the fluctuation level is reduced compared with the one before the kick [Fig. 8(a)]. By that turn number ($N=1000$), large scale fluctuations which correspond to lower mode numbers have been removed. The higher mode numbers in the power spectrum are dominant for the correction of smaller scale fluctuations. The turn number dependence of the laser power is illustrated in Fig. 10, for the $m=15$ mode 10(a) and the $m=45$ higher harmonic 10(b). Since the fluctuation pattern of the beam changes turn by turn, each mode amplitude shows stochastic oscillations. Each mode amplitude is also found to decrease with cooling by an almost exponential dependence in correction with the beam emittance (Fig. 7).

Figure 9(c) shows the difference of the power in each mode after $P_m^{(a)}$ and before $P_m^{(a)}$ the kick $\delta P_m\equiv P_m^{(a)}-P_m^{(b)}$. Due to the kick by the beat wave, the fluctuations are found to be reduced. As seen in Fig. 9(b), more laser power is

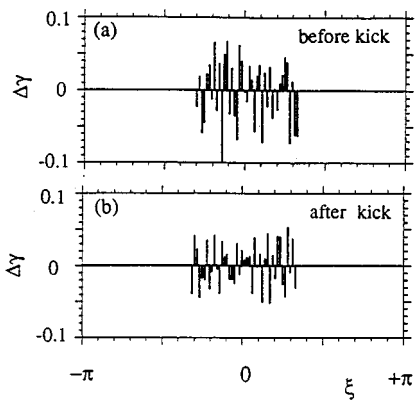

FIG. 8. (a) and (b) are fluctuation pattern $\langle\delta\gamma\rangle_j/\overline{\gamma}$ of the beam before and after the kick, at the kick at turn $N=1000$.

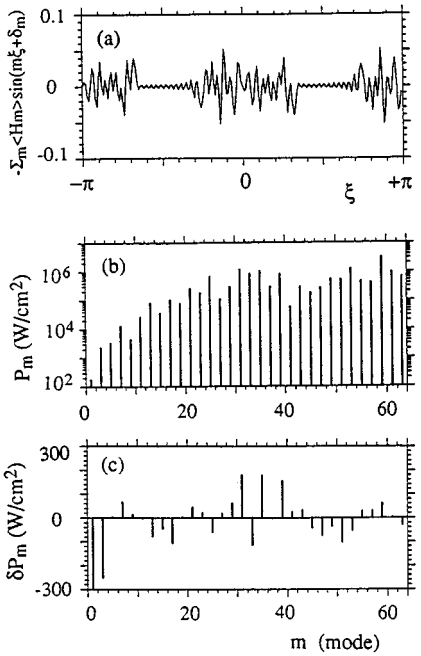

FIG. 9. The beat wave pattern (a) at turn $N=1000$ is shown. The power spectrum of laser field (b) at turn $N=1000$, and (c) the difference of laser power in each mode after $P_m^{(a)}$ and before $P_m^{(b)}$ the kick ($\delta P_m \equiv P_m^{(a)} - P_m^{(b)}$).

required for higher mode numbers for correction of smaller scale fluctuations. Furthermore, it is notable that while the change in the laser power spectra is small but finite ($|\delta P_m| \sim 1-300$ W/cm^2) and, in fact, can be used as a diagnostic tool for next kicks, the change in the total laser power before and after the kick and, thus, the overall power consumption are extremely small. This result indicates that cooling takes place by exchanging the fluctuations and randomness in the beam particles with the laser fields by simply rearranging the power spectra. Resultantly, the beam entropy

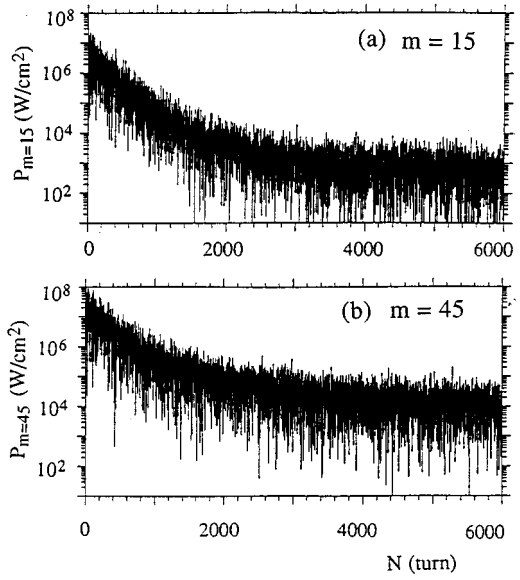

FIG. 10. Turn number dependence of laser power of the (a) $m=15$ mode and (b) the $m=45$ higher harmonic.

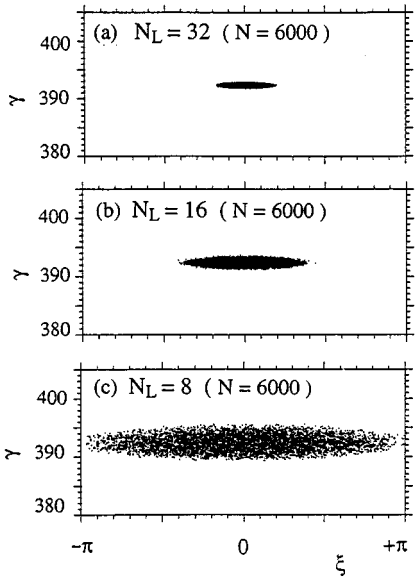

FIG. 11. Particle distribution plot of the beam after $N=6000$ turns when (a) 32 odd harmonic lasers ($m=1-63$), (b) 16 odd harmonic lasers ($m=1-31$), and (c) 8 odd harmonic lasers ($m=1-15$) are employed.

is transferred to the laser fields during the interaction and then the scattered laser (or photon) entropy is increased, as we discuss in Sec. IV B.

Here, we investigate the dependence of the cooling efficiency on the number of higher harmonics of the laser. In Fig. 11, we show a particle distribution plot of the beam after $N=6000$ turns when we employed 16 odd harmonic lasers ($m=1-31$) [Fig. 11(b)] and 8 odd harmonic lasers ($m=1-15$) [Fig. 11(c)] which correspond to $n=64$ and $n=32$ slices in the phase space, respectively. The turn number dependence of the emittance for the 16 and 8 harmonic laser cases are also shown in Fig. 7. It is found that the cooling rate and/or efficiency strongly depends on the number of harmonic lasers and the slice which corresponds to the precision of the beam diagnostics in the phase space. As discussed in Sec. III D, the ideal kick is also modified by the change of the wave number of laser when the beam current and/or density becomes higher. In Fig. 12, the turn number dependence of the emittance for the case of an average beam

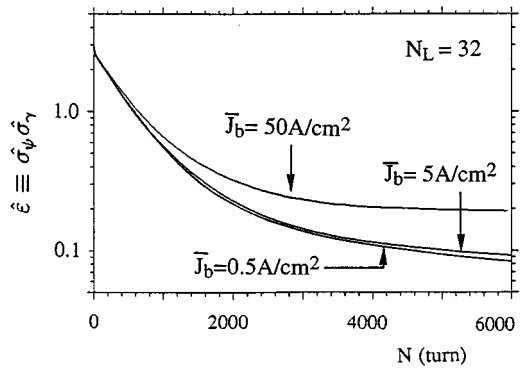

FIG. 12. Emittance $\hat{\varepsilon} \equiv \sigma_\psi \sigma_\gamma / \pi \gamma_b$ as a function of turn N for slice number $N_L=32$ with beam current $J_b=0.5$ A/cm^2, 5 A/cm^2, and 50 A/cm^2.

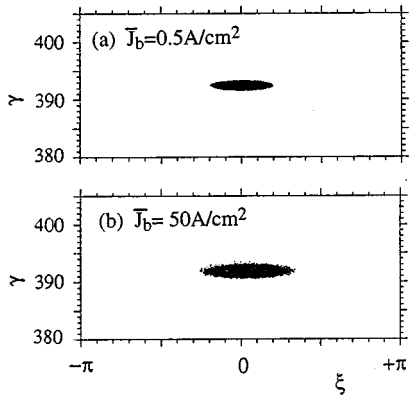

FIG. 13. Particle distribution plot at $N=6000$ turns for current (a) $\bar{J}_b=0.5$ A/cm^2 and (b) 50 A/cm^2.

current of $\bar{J}_b=0.5$, 5.0, and 50 A/cm^2 are also shown. Note that the map, $\mathcal{M}(K;P)$, phase space rotation angle per interaction is different from previous cases to accentuate the differences between the 0.5, 5.0, and 50 A/cm^2 cases. The particle distribution plot at $N=6000$ turns is shown in Fig. 13(b). Although the initial cooling rate which shows an exponential dependence does not change as seen in Fig. 12, it is found that the cooling efficiency after $N=1000-1200$ becomes lower and is almost saturated. The decrease of the cooling efficiency is considered as follows. In the present method strong cooling of the beam is accompanied with contraction in the phase direction and the beam density becomes higher. As a result, the interaction between laser field and beam particles becomes strong and the laser field pattern, which is initially adjusted, is modified during the kick due to the change in the wave number δk_m in Eq. (45). In the present case, a laser field with the lower mode number ($m=1-15$) is found to gain energy from the beam particles. Then, the ideal kick of the beam which leads to cooling is prevented.

B. Laser phase space

In Fig. 14, we show the laser phase space where the change of laser phase ϕ_m and amplitude a_m for one turn obtained from Eqs. (30) and (31), $(\Delta\phi_m,\Delta a_m/a_m)$, are plotted at $N=500$ [14(a)] and $N=5000$ [14(b)] for the $N_L=32$ case. When the irradiated laser structure is in a reasonable match with the internal structure of the beam (to the mth order), rapid cooling of the beam and rapid entropy increase of the laser light simultaneously take place, a resonance phenomenon of entropy. This is also confirmed in Fig. 14(c) which illustrates the turn number dependence of the root mean square (rms) of the phase space distribution $\sigma_L\equiv\sigma_a\sigma_\phi[(\sigma_a,\sigma_\phi)$: rms in $(\Delta\phi_m,\Delta a_m/a_m)]$, showing an opposite dependence from that of the beam emittance [Fig. 7]. Namely, the reaction of the laser fields with the beam increases with a decrease of the beam emittance, indicating a *diminishing return* in the cooling system. Note that the increased laser entropy is taken out from the system on each turn because the laser fields are renewed turn by turn based on the beam fluctuation diagnostics. In Figs. 15, we also show $(\Delta\phi_m,\Delta a_m/a_m)$ plot for $N_L=32$ [15(a)] and $N_L=8$ [15(b)] for different values of the field strength parameter

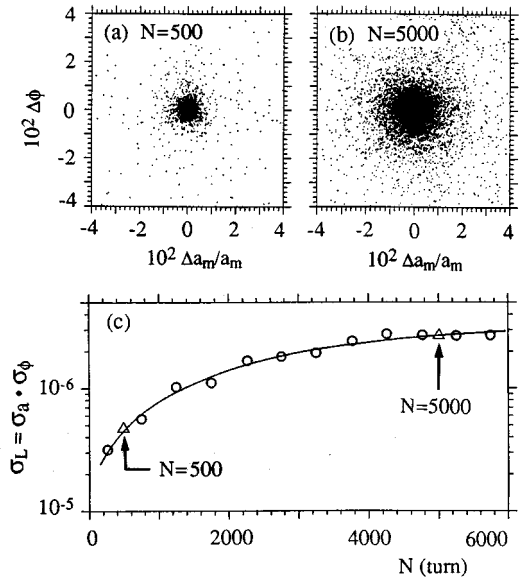

FIG. 14. Plot of $(\Delta\phi_m,\Delta a_m/a_m)$ at turn $N=500$ (a) and $N=5000$ (b) for $N_L=32$ case. To increase the statistical accuracy, $(\Delta\phi_m,\Delta a_m/a_m)$ over the region $250\leqslant N\leqslant 750$ (a) and $4750\leqslant N\leqslant 5250$ are simultaneously plotted. (c) Turn number dependence of the effective laser interaction temperature $\sigma_L\equiv\sigma_a\sigma_\phi$.

α in Eq. (43), i.e., $\alpha=1.0$(I) and $\alpha=2.5$(II). Note that the value of α larger than $\alpha=2$ provides an over kick as discussed in Eq. (43). Even though the individual phase and amplitude are tuned, if they are over kicking, as demonstrated in (II) in Fig. 15(a) and 15(b), no significant heating of the laser and therefore no significant cooling of the beam as a whole takes place. In the conventional wave-particle interaction, when the wave is in resonance with particles (''the wave-particle resonance''), energy exchange ΔE between the wave and particles takes place. However, entropy exchange ΔS may or may not take place. For example, in the simple case of Landau damping of a single small amplitude

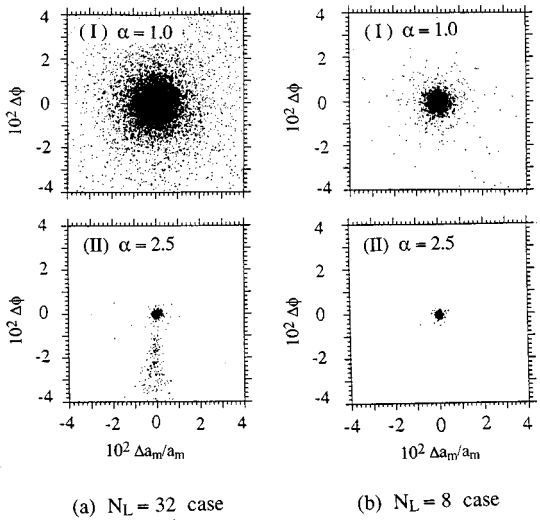

FIG. 15. Plot of $(\Delta\phi_m,\Delta a_m/a_m)$ during $1\leqslant N\leqslant 5000$ for different value of field strength parameter $\alpha=1$ (I) and $\alpha=2.5$ (II) in the case of $N_L=32$ (a) and $N_L=8$ (b).

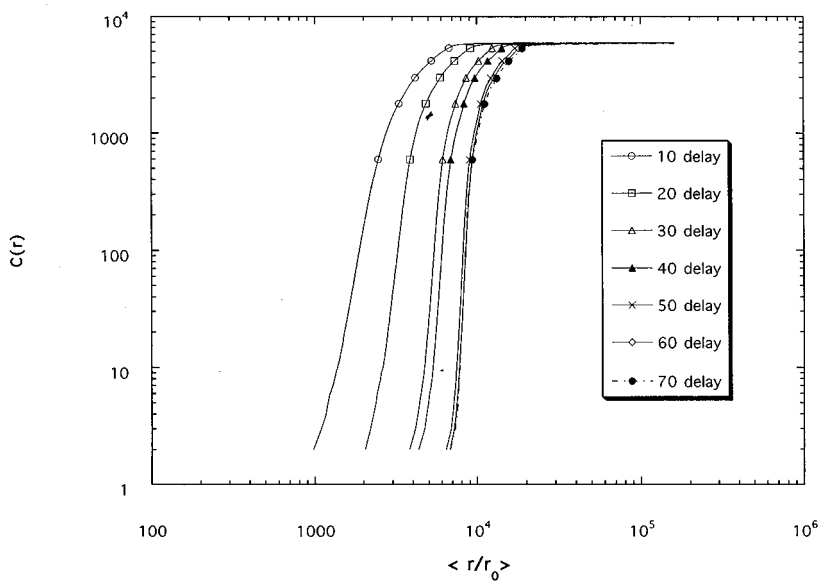

FIG. 16. The correlation integral, $C(r)$, is plotted for various delay vectors consisting of $(\Delta\phi_m, \Delta a_m/a_m)$ for the longest wavelength mode $(m=1)$.

wave, we note that $\Delta E \neq 0, \Delta S \simeq 0$, and thus $|\Delta S/\Delta E| \simeq 0$. On the other hand, in our case when the wave structure is well matched with the internal phase space structure of the particle beam, even though the energy exchange between the waves and particles is negligible $(\Delta E \sim 0)$, a large amount of entropy exchange $(\Delta S \neq 0)$ may take place, i.e., $|\Delta S/\Delta E| \sim \infty$. We call this later phenomenon *entropy resonance* (in contrast to the conventional wave-particle energy resonance).

Next we examine the dimensions of the scattered light when cooling occurs in the beam. This is done by calculating the dimensionality of the attractor of the time series of $(\Delta\phi_m, \Delta a_m/a_m)$. The dimension of the attractor indicates the degrees of freedom of the system needed to specify the state of the system [19]. It is the number of degrees of freedom realized by the dynamics as opposed to the underlying physical degrees of freedom [19].

To calculate the dimensionality of the attractor for a time series we use a variation of the method of Grassberger and Procaccia [20,21]. In this method one calculates the correlation integral $C(r)$

$$C(r) = \lim \frac{1}{N^2} \times \{ \text{number of pairs } (i,j) \text{ whose distance } |\mathbf{X}_i - \mathbf{X}_j| \text{ is less than } r \}, \quad (50)$$

where the m dimensional delay vectors $\mathbf{X}_i$ and $\mathbf{X}_i$ are constructed from the time series

$$\mathbf{X}_i = (f(t_i), f(t_i-\tau), f(t_i-2\tau), f(t_i-3\tau), \ldots, f(t_i-m\tau)), \quad (51)$$

$$\mathbf{X}_j = (f(t_j), f(t_j-\tau), f(t_j-2\tau), f(t_j-3\tau), \ldots, f(t_j-m\tau)), \quad (52)$$

where the indices i,j refer to different times in the time series. The dimension m of the vectors $\mathbf{X}_i, \mathbf{X}_j$ must be greater than the dimension of the attractor. We want to find a power law of the form

$$C(r) \approx (r)^{\nu}, \quad (53)$$

where ν is dimension of attractor. To find the exponent ν of a particular curve we calculate a local value of the slope of $\ln(C)/\ln(r)$ between neighboring points [19]. To find the dimension of the time series one increases the dimension of the vectors $\mathbf{X}_i, \mathbf{X}_j$ until the calculated dimension approaches some asymptotic limit. It has been shown that because of artifacts in this measurement technique, it is a rough measure of the underlying dimensionality of a system, but one can tell at least whether the system is completely random or very low dimensional [19]. For purely random noise ν increases without bound as the dimension of the vectors $\mathbf{X}_i, \mathbf{X}_j$ are increased.

We calculate the dimension of the time series of $(\Delta\phi_m, \Delta a_m/a_m)$ for the shortest and longest laser modes of a total of 32 modes used to cool the beam where a total of 5184 simulation particles is used. The time series for each mode consists of 6000 data points. Figure 16 shows a plot of $C(r)$ for various delay vector lengths for the longest mode used to cool the beam. It is apparent that there is not a single power law which describes the curves. It is known that strange attractors have a wider range of scaling properties than can be described by a single exponent [19]. The curves level off for large r due to the finite length of the time series. Figure 17 shows the local slope for each of the different delay curves in $\ln[C(r)]/\ln(r)$. It is apparent that as the delay is increased the local slope also increases until the number of delay vectors is 50. At this point the curves for 50, 60, and 70 delay vectors converge. The curves indicate that the maximum dimension is between 30 and 40. For the shortest wavelength mode the local slope $\ln[C(r)]/\ln(r)$ increased without bounds as the delay was increased indicating that the dimension of the time series was close to that of white noise. The reason for this difference in the dimensions between the modes is the fact that the beam has been cooled substantially. To the long wavelength mode the beam looks more like a single particle and, therefore, the dimensionality reflects the number of laser wave modes used to kick the system. In this case 32 modes were used. When we calculate the dimensionality of the system using the shortest wave mode, more of the fine scale internal structure of the beam is seen. On this finer

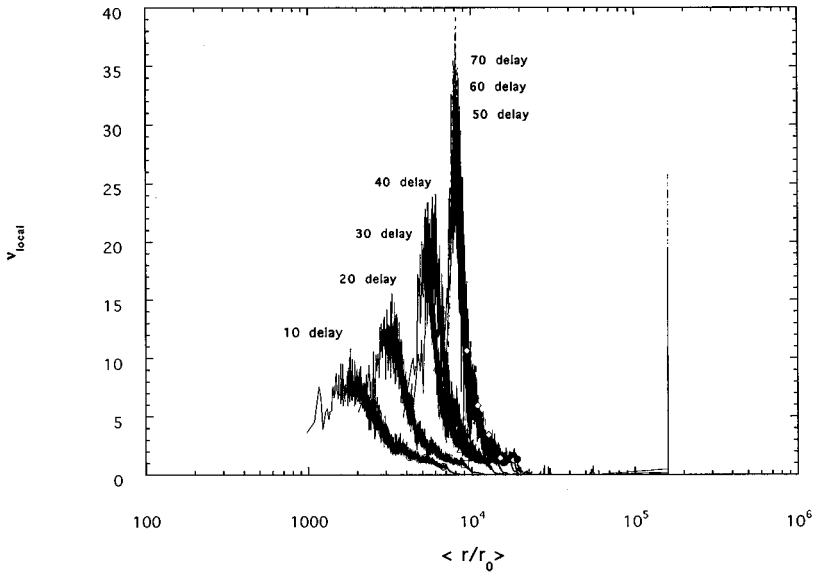

FIG. 17. Local power law fit for the longest wavelength mode to $C(r)$ for the various delay vectors vs $\langle r/r_0 \rangle$, where r_0 is an arbitrary normalization distance, ν is the power law exponent, and the embedding dimension is twice the number of delay points used, since both $(\Delta\phi_m, \Delta a_m/a_m)$ are used. The dimension is determined when curves of different delays converge to the same values. Convergence occurs between 50 and 70 delay points giving $\nu \approx 30$–40.

scale the actual degrees of freedom of the beam from the number of particles in the system is reflected. High dimensionality for the shortest mode indicates that it is still useful for cooling. It indicates that there are fluctuations which can be eliminated. The low dimensionality of the longest mode reflects that cooling is hard to perform since internal fluctuations have been eliminated at these scale lengths. It is apparent that as the emittance of the beam is reduced the dimensionality measured by the short and long wave mode should approach each other and simply reflect the input degrees of freedom from the laser light. Physically, if the beam had been cooled to zero emittance, then it would look like a single particle of charge N, where N is the number of particles in the beam. When the beam is a point particle, all the laser modes cannot make any internal structural changes to the beam. Since the beam is kicked by the incoming laser light, the dimensionality or degrees of freedom of its motion is determined by the number of modes input.

When the particle number of the simulation is increased by four times a slower cooling time and, therefore, larger emittance for the beam after the same number of kicks, 6000 is observed. For the longest mode we get a dimension of around 25 to 30 and for the shortest mode we get a dimension of around 60 to 70. To the long wavelength mode the beam again looks more like a single particle and, therefore, the dimensionality reflects the number of laser wave modes used to cool the system. When we calculate the dimensionality of the system using the shortest wave mode, more of the fine scale internal structure of the beam is again seen. However, in this case on this finer scale the fluctuation level is lower due to the larger number of particles. The random fluctuations or coarse grained structure has been pushed to a smaller scale size due to the addition of particles. On the same scale length compared with fewer particles the phase space looks more ''fluid'' like. So the dimension measured for this mode is less than that measured in the previous simulation.

We can further analyze the characteristics of the scattered laser light by looking at the entropy of the light. The correlation dimension of the time series of the scattered laser light can be related to the concept of higher-order entropy Eq. (7) through the Kolmogorov entropy [22]. First we need to define a quantity K_n as

$$K_n = -\sum_{i_0,\ldots,i_n} P_{i_0,\ldots,i_n} \ln P_{i_0,\ldots,i_n} \tag{54}$$

where $P_{i_0,\ldots,i_n}$ is the joint probability that a trajectory $\vec{x}(t)=[x_1(t),\ldots,x_d(t)]$ in a d-dimensional space which has been partitioned into boxes of size l^d, where l is the precision, follows the sequence $\vec{x}(t=0)$ is in box i_0, $\vec{x}(t=\tau)$ is in box $i_1,\ldots,$ and $\vec{x}(t=n\tau)$ is in box i_n. This quantity K_n is the discrete time dependent equivalent of the higher-order entropy, S_n, in Eq. (7) where the phase space variables are replaced by points in a time series. The Kolmogorov entropy is then defined by

$$K = \lim_{\tau\to 0}\lim_{l\to 0}\lim_{N\to\infty} \frac{1}{N\tau}\sum_{n=0}^{N-1}(K_{n+1}-K_n), \tag{55}$$

$$= -\lim_{\tau\to 0}\lim_{l\to 0}\lim_{N\to\infty} \frac{1}{N\tau_{i_0,\ldots,i_N}} \sum_{i_0,\ldots,i_N} P_{i_0,\ldots,i_N} \ln P_{i_0,\ldots,i_N}, \tag{56}$$

where it is defined as the average rate of loss of information. For regular motion $K=0$, for chaotic motion $K>0$, and for random motion $K\to\infty$. In practical terms the K entropy is difficult to calculate. However, a much easier quantity to calculate, known as the K_2 Renyi entropy is related to the correlation integral $C_d(\epsilon)$ calculated previously [23]

$$K_{2d}(\epsilon) = \frac{1}{\tau}\ln\frac{C_d(\epsilon)}{C_{d+1}(\epsilon)}, \tag{57}$$

$$K_2 = \lim_{\substack{d\to\infty \\ \epsilon\to 0}} K_{2d}(\epsilon), \tag{58}$$

where d is the dimension of the space in which the correlation integral is calculated, ϵ is the size of the region of phase

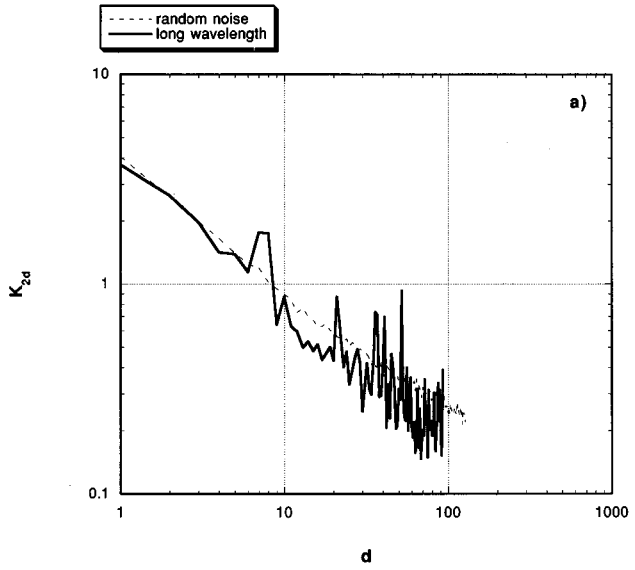

FIG. 18. Maximum K_{2d} entropy plotted vs the dimension d for (a) long wavelength and (b) short wavelength. White noise is plotted for comparison.

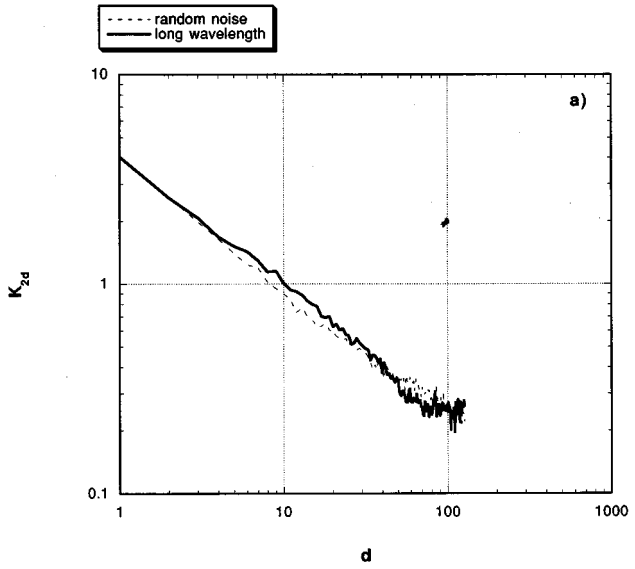

FIG. 19. Maximum K_{2d} entropy plotted vs the dimension d for (a) long wavelength and (b) short wavelength $\alpha=2.3$ (no cooling). White noise is plotted for comparison.

space, and ν is the correlation exponent which characterizes the dimension of the attractor. It has been shown that

$$K_2 \leqslant K \tag{59}$$

and for typical cases is numerically close [23].

In Figure 18 we show the maximum K_{2d} entropy calculated using Eq. (57) from the correlation function $C_d(\epsilon)$ for all values of ϵ versus the dimension d. The two cases shown are from a cooling simulation for the long wavelength [18(a)] and short wavelength [18(b)] laser modes. We plot the K_{2d} entropy calculated for white noise as a comparison. It can be seen that as the dimension d is increased the entropy decreases for all three cases. The K_{2d} entropy indicates the rate at which information is lost or, in our case, the rate at which information is extracted by the laser beam. Low values indicate that information is being extracted at a slow rate, whereas high values indicate a fast rate of information extraction (fast cooling). As is apparent from the figure the short wavelength laser is extracting information at the fastest rate. Another feature is the structure in both the long wavelength and short wavelength entropy. The white noise entropy smoothly decreases with increasing dimension, whereas the scattered laser light shows jumps in the entropy. For some values the entropy extraction rate is very high. In Fig. 19 we show the maximum K_{2d} entropy versus the dimension d for the long wavelength [19(a)] and short wavelength [19(b)] for a noncooling case [$\alpha=2.3$ in Eq. (44)]. We plot the cases versus calculation of the maximum K_{2d} entropy for white noise. It is interesting to note that for the long wavelength mode the entropy nearly overlaps the entropy calculated for white noise. Also the corresponding lack of structure is apparent. In the short wavelength case there is still structure, indicating that cooling is still occurring for the short wavelength mode. This would not have been apparent only using the usual one-body entropy calculation.

V. ENTROPY AND COOLING

We summarize some of the findings in the computer simulation of our cooling method by arranging the laser modes to manipulate the inner structure of the beam in Sec. IV as follows.

(1) When cooling of the electron bunch takes place (Fig. 6), reduction of the area in phase space of the electron bunch is accomplished by an increase of the area in phase space of the laser photons [Fig. 14 and Fig. 15(I)]. This happens when the imposed laser pattern, $\{(a_m,\phi_m)\}$ is matched well with the internal structure of the beam. On the other hand, if we choose the laser to over kick (α greater than 2), the matching is not good and neither the reduction of the area in beam phase space or the increase of that of the laser photons occurs as much as in the above case [Fig. 15(II)].

(2) As shown in Fig. 7, the cooling time sensitively depends on the number of colors (modes) of the laser imposed: the greater the number of colors, the quicker the cooling is. This means that the finer the detail of phase space is resolved and thus manipulated, the faster the reduction of the phase space volume is.

(3) As the number of turns of the electron bunch in the ring increases and its cooling proceeds, the increase in the area in the phase space of the laser light becomes greater [Fig. 14(c)], while the decrease of the area in phase space of the beam slows down (Fig. 7). This means that it becomes more difficult to cool cooler beams and takes more effort (and thus entropy) to accomplish the same amount of cooling.

(4) The dimension of information contained in light scattered off the beam is dependent on how much cooling has taken place. The dimension associated with short wavelength light is greater than that with longer one and it asymptotes toward the number of independent modes of laser light that are imposed externally by our algorithm. This means that the scattered light sees detailed dynamics of internal structure that is coarse grained from the system of N individual particles down to the number of degrees of freedom that is roughly equal to the dimension. The shorter the laser wavelength, the more minutely it can resolve in phase space.

(5) When the higher dimensional entropy of the scattered laser light is calculated, it is found that when cooling occurs, there is structure. That is, the entropy fluctuates with dimension whereas white noise smoothly decreases with increasing dimension. When no apparent cooling is occurring, the entropy calculated from the scattered laser loses the structure at long wavelengths, but some structure is still present at short wavelengths.

These phenomena are all related to the internal structure of system of charged particles and photons. In order to characterize these phenomena theoretically and to formulate mathematically, we analyze the dynamics in terms of μ space (six-dimensional phase space) and Γ space ($6\times M$ dimensional phase space, where M is the dimension of appropriate degrees of freedom or ''particles''). We introduce $6M$-dimensional Γ space and its dynamics for the description of μ-space internal dynamics. The volume reduction in phase space of μ space corresponds to the reduction of dimensions of phase space of Γ space. Once we introduce Γ space, it is straightforward to introduce higher-order correlation and related higher-order entropy.

The reason why we need to introduce such a tool may be illustrated by the following simplified example of magnetic tapes [13]. Think of a bad quality tape which contains noise. This tape does not contain information. Think of another tape which contains a poem. This tape contains a large amount information of high quality. Consider a third tape which is blank. This tape contains no information, but is coherent. According to Shannon's entropy [24] which is discrete equivalent to the one-body entropy in Eq. (6) (related to the one-body distribution function) and is a measure of information, the entropy of the noisy tape and that of a poem are high. Shannon's entropy cannot distinguish the information of the noisy tape (useless or none) and the poetic tape (useful and rich). One may also argue that both the blank tape and poetic tape are coherent, while the noisy tape is incoherent. Once again Shannon's entropy fails to carry such a distinction. In order to remedy this difficulty, higher-order entropies, based on higher-order correlations, have been introduced [13]. These quantities are based on Γ-space quantities and dynamics (and their distribution functions $\mathcal{D}$ or f_n). The usefulness of the higher-order entropies is made apparent in our calculation of the K_2 entropy. By calculating this quantity the noisy tape, blank tape, and tape with poetry can be easily distinguished by examining the variation of K_2 with increasing dimension (longer correlation times). When we examine the scattered laser light, random white noise can be distinguished from cases where cooling is occurring due to the structure observed at higher correlation dimensions. Particularly in the case of overkicking, the distinction from white noise is only apparent when the higher dimensional entropy is calculated [see Fig. 19(b)].

The probability distribution function in Γ space for N ''particles'' (or $6N$ degrees of freedom) is given by $\mathcal{D}\mathbf{u}\equiv f_N(q_1,p_1,q_2,p_2,\ldots,q_N,p_N,t)$ as in Sec. I. Cooling, the reduction of the area (or volume) of phase space in μ space, corresponds to a ''bundle up'' of scattered vectors in Γ space. If this bundle up loses spread in one (or more) particular direction(s), this corresponds to losing of dimensions in Γ space. When the cooling proceeds in our measurement in Sec. IV, the dimension of the laser light has reduced.

Another way to look at the higher-order entropies from a phase space point of view is as a representation of the beam emittance in higher dimensions. As was mentioned in the beginning of Sec. I the logarithm of the beam emittance is related to the entropy. The higher-order entropies S_n in Eq. (7) are determined from f_n the n body distribution function. The function f_n can be thought of as a function in a higher dimensional space. One can imagine this as having an analogous higher dimensional emittance ϵ_n where n is the dimension of the space. In the case where we go to the $6N$-dimensional γ space the distribution function is a single point and the corresponding high dimensional emittance ϵ_{6N} and, therefore, the higher-order entropy S_{6N} in that space is zero. As we go to lower and lower dimensional spaces the corresponding emittance and higher-order entropy increase. In six-dimensional phase space (μ space), where the equations of motion are integrated over $6N-6$, coordinates, we obtain the usual emittance and entropy. As we cool a charged particle beam consisting of N particles the area in μ space reduces. Correspondingly, the higher dimensional emittances

and higher-order entropies also decrease. Essentially, cooling of a N particle system is pushing the single point distribution function in the $6N$-dimensional space down to progressively lower dimensions. One can see that when a N particle system is cooled to its limit the entire distribution looks like a single point in six-dimensional phase space (μ space).

The observation that more rapid cooling with more colors (or degrees of freedom) of illuminated laser may be termed as the greater change in (specific) higher-order entropy per energy. In other words for a given change of energy δE, the modulus of the change of the entropy δS_n is greater for greater n

$$\left|\frac{1}{n}\frac{\partial S_n}{\partial E}\right| > \left|\frac{1}{m}\frac{\partial S_m}{\partial E}\right|, \tag{60}$$

for $n>m$, where S_n was defined in Eq. (7). Note that for $m=1$ for the dynamical system with temperature T we know the familiar result

$$\frac{\partial S_1}{\partial E} = \frac{1}{T}, \tag{61}$$

i.e., the change in the one-body (usual or the lowest order) entropy per energy is equal to the inverse temperature. That is, a greater change in entropy per energy can be achieved in a colder system; an intuitively reasonable interpretation can be rendered. A rigorous mathematical proof of Eq. (60) has been carried out by Wolf [25], in which a simple Ising model was adopted. In this system it can be shown that

$$\frac{1}{n}\frac{\partial S_n}{\partial E} = \left(1-\frac{1}{n}\right)\frac{\partial S_I}{\partial E}, \tag{62}$$

where $S_I \equiv \lim_{n\to\infty}(S_n/n)$. Thus $(1/n)(\partial S_n/\partial E)$ is greater for greater n in the Ising system. In Fig. 6 of our cooling simulation when we employ a large number of colors, i.e., a large dimension in laser phase space, the cooling is rapid and though the employed laser power may be considerable, the expended laser energy summed over all colors is far smaller than that needed for an individual laser light. We believe that this is an observation of this principle, Eq. (62).

In this paper we have introduced a general method for the phase space control of charged particle beams. We have concentrated on the properties of cooling a charged particle beam and the method of kicking the beam given that a feedback system with high enough resolution of the phase space of the beam is possible. We have not addressed the problem of extracting the phase space information which in and of itself represents a formidable task. One of the problems is that of the large bandwidth (in our example in the text it is about 10 THz [28]), which requires excellent diagnostics and computational techniques. Related to this problem is the obfuscation of the beam data arising from the incomplete understanding of accelerator structures. For simple manipulations of the beam phase space not involving cooling such as beam shaping or bunching where the resolution and feedback constraints are greatly relaxed currently available techniques such as tomography [29], or other methods can be used. In our next paper we will address this problem by looking at modern techniques of mapping the phase space distribution from the synchrotron radiation reconstruction [16], time of flight methods [11], and other recent progress [26]. In addition, we are developing feed-forward neural net prediction algorithms, based on (i) the inversion from the phase space moments [17], (ii) the prediction of the observed beam fluctuations, and (iii) the inversion from the scattered laser light, an approach similar to Ref. [27]. In the future we need to investigate a more rigorous (and orthogonal) treatment of the phase space of photons. We then need to mathematically formulate the observed phenomenon of entropy resonance, which is conceptually distinct from the conventional wave-particle resonance. We further need to mathematically formulate the ''law of diminishing returns'' in terms of higher-order entropy. These tasks may be repended ones to build a foundation of structural statistical mechanics as opposed to the conventional (thermodynamical) statistical mechanics. We envisage that further studies in cooling of charged particles beams via lasers will bring in not only a novel and, perhaps, more efficient cooling technique, but also allow us to learn the dynamics and needed mathematical tools to analyze the internal structure of Γ space for the manipulation of the beam phase space.

ACKNOWLEDGMENTS

This work was supported by JAERI and in part by the U.S. DOE. We would like Professor M. Date for his continued support of this project.

[1] S. van der Meer, CERN Report No. PS/AA/78-2, 1978 (unpublished).

[2] S. van der Meer, CERN Report No. PS/AA/78-6, 1978 (unpublished).

[3] A. W. Chao, *Physics of Collective Beam Instabilities in High Energy Accelerators* (Wiley, New York, 1993).

[4] S. Chattopadhyay, in *The Future of Accelerator Physics: The Tamura Symposium Proceedings*, edited by T. Tajima, AIP Conf. Proc. No. 356 (AIP, New York, 1996), p. 15.

[5] G. I. Budker, in *Proceedings of the International Symposium on Electron and Positron Storage Rings, Saclay, 1966*, edited by H. Zyngier and E. Crémeaux-Alean (PUF, Paris, 1967), p. 11–1-1; G. I. Budker *et al.*, Part. Accel. **7**, 197 (1976).

[6] D. Neuffer, Part. Accel. **14**, 75 (1983).

[7] M. Sands, The Physics of Storage Rings an Introduction, SLAC-121 UC-28 (ACC), 1970; M. Sands, in *Proceedings of the International School of Physics, Varenna, 1969*, edited by B. Touschek (Academic, New York, 1971).

[8] S. V. Andreev, V. I. Balykin, V. S. Letokhov, and V. G. Minogin, Pis'ma Zh. Éksp. Teor. Fiz. **34**, 463 (1981) [JETP Lett. **34**, 442 (1981)]; W. D. Phillips and H. Metcalf, Phys. Rev. Lett. **48**, 596 (1982).

[9] S. Schröeder *et al.*, Phys. Rev. Lett. **64**, 2901 (1990).

[10] D. Möhl, G. Petrucci, L. Thorndahl, and S. van der Meer, Phys. Rep. **58**, 73 (1980).
[11] M. S. Zolotorev and A. A. Zholents, Phys. Rev. E **50**, 3087 (1994).
[12] J. Bisnagno and C. Leeman, in *Physics of High Energy Particle Accelerators*, edited by R. A. Carrigan, F. R. Huson, and M. Month, AIP Conf. Proc. No. 87 (AIP, New York, 1982), p. 583; J. Bisnagno, in *Physics of High Energy Particle Accelerators*, edited by M. Month, P. F. Dahl, and M. Dienes, AIP Conf. Proc. No. 127 (AIP, New York, 1983), p. 443.
[13] T. Tajima, *Computational Plasma Physics: With Applications to Fusion and Astrophysics* (Addison-Wesley, Reading, MA, 1989).
[14] T. Tajima and J. M. Dawson, Phys. Rev. Lett. **43**, 267 (1979).
[15] Y. Kishimoto, H. Oda, and M. Shiho, Phys. Rev. Lett. **65**, 851 (1990).
[16] A. Ogata, T. Mitsuhashi, T. Katsura, N. Yamamoto, and T. Kawamoto, in *Proceeding of the IEEE Particle Accelerator Conferences, 1989*, edited by F. Bennett and J. Kopta (IEEE, New York, 1989), Vol. 3, p. 1498.
[17] J. Koga and T. Takeda, Nucl. Instr. Meth. Phys. Res. Sec. A **363**, 580 (1995).
[18] α is usually taken to be less than two to prevent the over kicking.
[19] N. A. Gershenfeld, Physica D **55**, 135 (1992).
[20] P. Grassberger and I. Procaccia, Physica D **9**, 189 (1983).
[21] Y. Termonia and Z. Alexandrowicz, Phys. Rev. Lett. **51**, 1265 (1983).
[22] J. D. Farmer, Z. Naturforsch. Teil A **37**, 1304 (1982).
[23] P. Grassberger and I. Procaccia, Phys. Rev. A **28**, 2591 (1983).
[24] C. E. Shannon and W. Weaver, *The Mathematical Theory of Communication* (University of Illinois Press, Champagne, 1949).
[25] D. R. Wolf, Ph.D. thesis, University of Texas, Austin, 1996.
[26] J. Pasour and M. Ngo, Rev. Sci. Instrum. **63**, 3027 (1992).
[27] A. A. Mikhailichenko and M. S. Zolotorev, Phys. Rev. Lett. **71**, 4146 (1993).
[28] Note that this figure is typically one order of magnitude smaller than the required bandwidth of optical stochastic cooling.
[29] C. T. Mottershead, IEEE Trans. Nucl. Sci. **NS-32**, 1970 (1985).